nature neuroscience

Coactivation and timing-dependent integration of synaptic potentiation and depression

Huai-Xing Wang[1], Richard C Gerkin[2,3,5], David W Nauen[2–5] & Guo-Qiang Bi[1–3]

Neuronal synaptic connections can be potentiated or depressed by paired pre- and postsynaptic spikes, depending on the spike timing. We show that in cultured rat hippocampal neurons a calcium/calmodulin-dependent protein kinase II (CaMKII)-mediated potentiation process and a calcineurin-mediated depression process can be activated concomitantly by spike triplets or quadruplets. The integration of the two processes critically depends on their activation timing. Depression can cancel previously activated potentiation, whereas potentiation tends to override previously activated depression. The time window for potentiation to dominate is about 70 ms, beyond which the two processes cancel. These results indicate that the signaling machinery underlying spike timing–dependent plasticity (STDP) may be separated into functional modules that are sensitive to the spatiotemporal dynamics (rather than the amount) of calcium influx. The timing dependence of modular interaction provides a quantitative framework for understanding the temporal integration of STDP.

In the mammalian brain, patterned neuronal activity leads to modification of specific synaptic connections[1], a process that is believed to be central to the development of precisely organized neuronal circuits as well as for learning and memory[2–4]. A hallmark of such activity-induced synaptic plasticity is that different activity patterns can lead to either strengthening or weakening of synapses, commonly known as long-term synaptic potentiation (LTP) or depression (LTD), respectively[4–7]. In traditional studies of homosynaptically induced plasticity, LTP is generally induced by bursts of high-frequency stimulation of input axons, whereas LTD is induced by low-frequency stimulation[5–7]. In the recently characterized STDP, the polarity of synaptic modification depends on the precise timing of individual pre- and postsynaptic spikes[4,8,9]: potentiation is induced if a postsynaptic spike repetitively follows a presynaptic spike by a few milliseconds, whereas depression is induced if the temporal order of the spike pairing is reversed[10–19]. Such sensitivity to activity patterns is crucial for the formation of specific engrams in neuronal circuits[20,21].

To what extent can a synapse precisely interpret incoming spike patterns? *In vivo*, a synapse experiences complex patterns of ongoing activity. Will the cellular processes involved in LTP and those involved in LTD both be activated when multiple pre- and/or postsynaptic spikes occur within milliseconds of one another? If so, how do these opposing processes interact to result in the final synaptic modification? Using cultured hippocampal neurons, we found that spike triplets or quadruplets could activate concomitantly a CaMKII-mediated potentiation process and a calcineurin-mediated depression process. The two modular processes integrated nonlinearly in a timing-dependent manner: depression canceled previously activated potentiation, whereas potentiation tended to override previously activated depression. The time window for potentiation to dominate is about 70 ms. In addition, blocking L-type calcium channels selectively suppressed depression, resulting in net potentiation. These results provide new quantitative rules for STDP integration. They also reflect the dynamic nature of the underlying cellular signaling.

RESULTS

Asymmetric temporal integration of STDP

Dual perforated whole-cell patch-clamp recordings were made on pairs of cultured hippocampal neurons, in which STDP has been demonstrated by repeated pairing of pre- and postsynaptic spiking at 1 Hz[13]. Based on the previously characterized spike timing window of STDP in these neurons, a potentiation (P) process can be triggered by a 'pre-post' spike pair (spike timing $t > 0$), whereas a depression (D) process can be induced by a 'post-pre' spike pair ($t < 0$). Here, P and D refer to the initial induction processes in the signaling pathways that lead to the final expression of STDP. In most studies and models of STDP, it is assumed that the spike pairing events in more complex spike patterns induce the P and D processes independently[18,19,22–27]. Under such an assumption, the simplest cases that could involve both potentiation and depression processes are triplet spiking paradigms (**Fig. 1**). For a triplet with a spiking sequence of pre-post-pre, P is presumably activated by the first spike-pairing event (pre-post) with spike timing t_1, and this is followed by D, which is activated by the second pairing (post-pre) with spike timing t_2. In a triplet case with post-pre-post spikes, the two processes are activated in the opposite temporal order. Hereafter, we use the two spike timing values $\{t_1, t_2\}$ to denote a triplet

[1]Department of Neurobiology, [2]Center for Neuroscience, [3]Center for the Neural Basis of Cognition and [4]Medical Scientist Training Program, University of Pittsburgh School of Medicine, Pittsburgh, Pennsylvania 15261, USA. [5]These authors contributed equally to this work. Correspondence should be addressed to G.Q.B. (gqbi@pitt.edu).

Published online 16 January 2005; doi:10.1038/nn1387

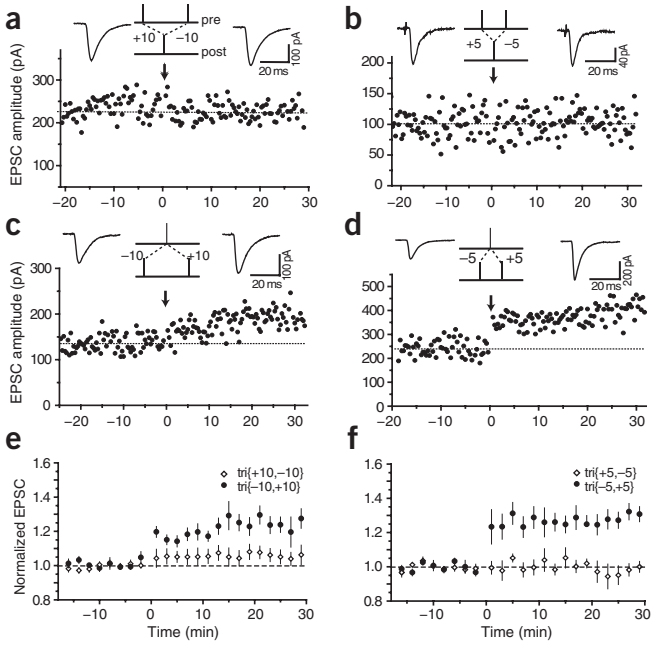

Figure 1 Triplet experiments showing asymmetric temporal integration of STDP. (**a**,**b**) Results from typical stimulation experiments with pre-post-pre triplets with (**a**) 10-ms and (**b**) 5-ms intervals. Data points show the peak amplitudes of monosynaptic EPSCs elicited by test stimuli (0.05 Hz) before and after repetitive triplet stimulation (arrow, 60 repetitions at 1 Hz during which the postsynaptic cell was under current clamp). Insets show traces of EPSCs (average of five consecutive events) 5 min before (left) and 20 min after (right) triplet stimulation. (**c**,**d**) Results from typical stimulation experiments with post-pre-post triplets with (**c**) 10-ms and (**d**) 5-ms intervals. (**e**) Summary of triplet experiments pre-post-pre {+10, –10} ($n = 12$) and post-pre-post {–10, +10} ($n = 7$). (**f**) Summary of triplet experiments pre-post-pre {+5, –5} ($n = 6$) and post-pre-post {–5, +5} ($n = 7$). Error bars, s.e.m.

paradigm; thus $t_1 > 0$ and $t_2 < 0$ for pre-post-pre triplets, whereas $t_1 < 0$ and $t_2 > 0$ for post-pre-post triplets.

We first examined the effects of triplet stimulation with spike timing intervals of ±10 ms. As in previous studies that used spike pairs[13], each triplet was repeated at 1 Hz during the 60-s induction period. In cultured hippocampal neurons, paired spiking with +10 ms spike timing induces significant LTP, whereas paired spiking with –10 ms timing induces significant LTD[13]. If P and D integrate linearly, as assumed in many STDP models[22–27], potentiation and depression in both pre-post-pre {+10, –10} and post-pre-post {–10, +10} paradigms should offset to result in the same outcome. Whereas no significant synaptic change was induced by the pre-post-pre triplet {+10, –10} (**Fig. 1a**,**e**), the post-pre-post triplet {–10, +10} did lead to marked LTP (**Fig. 1c**,**e**). We found similar results in experiments using triplets with intervals of ±5 ms (**Fig. 1b**,**d**,**f**). The amount of LTP that was induced by post-pre-post triplets (–10, +10; STDP ratio ± s.e.m., 1.27 ± 0.05) or (–5, +5; 1.28 ± 0.05) was similar to that induced by pre-post spike pairs alone (1.25 ± 0.05; see **Supplementary Fig. 1** online). It should be noted that the amount of LTP that was induced by pre-post spike pairs under these experimental conditions was lower than that reported in the previous study[13]. This is accounted for by the difference in initial synaptic strength, which significantly influences the degree of LTP induction[13]: on average, older cultures and stronger synapses were used in the current studies. Further, failure to induce significant change by the pre-post-pre triplets seemed to be due to active integration, because in the same experimental setting, post-pre spike pairs did result in LTD (**Supplementary Fig. 1**). Therefore, rather than summing linearly, the integration of potentiation and depression processes is temporally asymmetric: the two processes cancel when potentiation is triggered first, whereas potentiation dominates when it is triggered second.

Coactivation of kinase and phosphatase signaling modules

It is well established that protein kinases, especially CaMKII, are key to the induction of LTP by conventional tetanic stimulation paradigms, whereas phosphatases, including calcineurin and protein phophatase-1, are involved in LTD[28–33]. These pathways are likely to be involved in the induction of STDP by spike pairing with either positive (protein kinases) or negative (phosphatases) spike timing. They also may be coactivated by triplets or more-complex spike patterns. If this is the case, these pathways could be the molecular substrates for the proposed P and D processes that activate independently and then

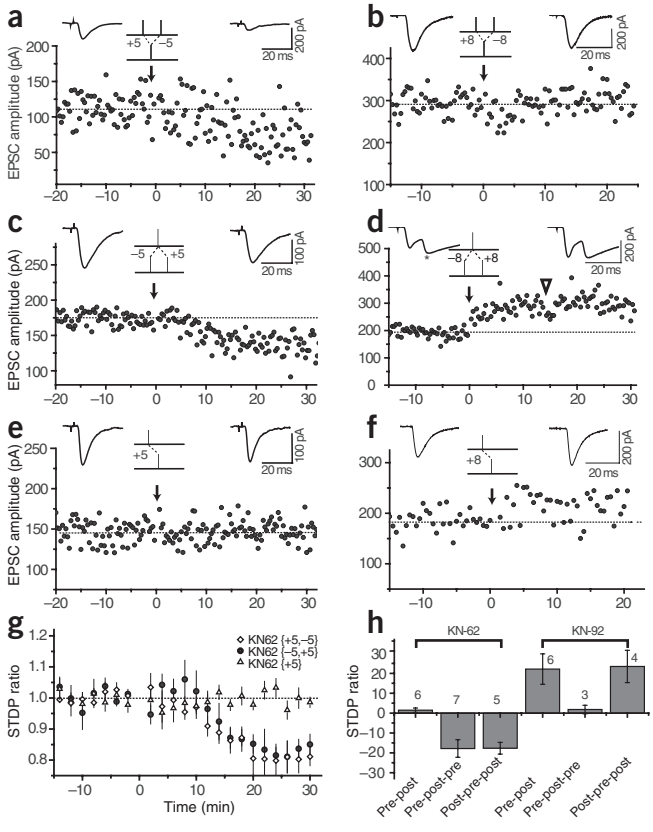

Figure 2 Effects of CaMKII inhibition on the induction and temporal integration of STDP. (**a**–**f**) The extracellular perfusion solution contained (**a**,**c**,**e**) the CaMKII antagonist KN-62 (10 μM; 5-ms intervals) or (**b**,**d**,**f**) the control analog KN-92 (10 μM; 8-ms intervals). (**a**,**b**) Results from typical experiments using pre-post-pre triplets. (**c**,**d**) Results from typical experiments using post-pre-post triplets. The synaptic response in **d** contained a GABAergic polysynaptic component (*). In this example, after the induction of LTP, a second time of stimulation (arrowhead) with pre-post-pre triplets did not induce any pronounced change. (**e**,**f**) Results from typical experiments using pre-post spike pair stimulation. (**g**) Summary of all experiments using triplet and pair stimulation in the presence of KN-62. (**h**) Summary of all experiments with KN-62 or KN-92. Number of experiments in each data set is shown above each column. Error bars, s.e.m.

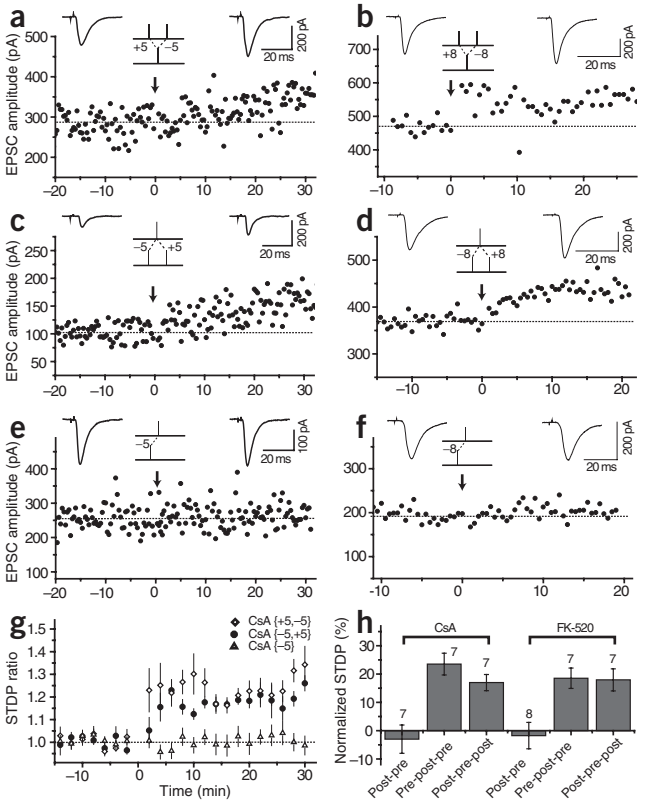

Figure 3 Effects of calcineurin inhibition on the induction and temporal integration of STDP. (**a**–**f**) Experiments were performed in the presence of (**a**,**c**,**e**) the calcineurin antagonist CsA (10 μM; 5-ms intervals) or (**b**,**d**,**f**) FK-520 (2.5 μM; 8-ms intervals). (**a**,**b**) Results from typical experiments using pre-post-pre triplets. (**c**,**d**) Results from typical experiments using post-pre-post triplets. (**e**,**f**) Results from typical experiments using post-pre spike pair stimulation. (**g**) Summary of all experiments using triplet and pair stimulation in the presence of CsA. (**h**) Summary of all experiments in CsA or FK-520. Number of experiments in each data set is shown above each column. Error bars, s.e.m.

integrate to result in net synaptic modification, as assumed in theoretical as well as experimental studies[18,19,22–26]. Indeed, in the presence of KN-62, a specific blocker of CaMKII[34], both triplets (pre-post-pre and post-pre-post) resulted in substantial depression (**Fig. 2a**,**c**,**g**,**h**). In contrast, in the presence of KN-92, an analog of KN-62 that does not inhibit CaMKII but has nonspecific inhibitory effects on voltage-gated K^+ channels similar to those of KN-62, the triplets led to either cancellation or LTP as in control conditions (**Fig. 2b**,**d**,**h**). As we had expected, KN-62, but not KN-92, also eliminated LTP that was induced by pre-post spike pairing (**Fig. 2e–h**). Notably, no significant LTD was observed in pre-post spike pairing experiments with the blockade of CaMKII. In the presence of cyclosporin A (CsA) or FK-520, blockers of calcineurin[32], both triplets induced pronounced potentiation (**Fig. 3a–d**,**g**,**h**). On the other hand, post-pre spike pairing in the presence of CsA or FK-520 resulted in neither LTP nor LTD (**Fig. 3e–h**). Therefore, the kinase and phosphatase pathways seem to be coactivated by either triplet paradigm, because blocking one pathway can unmask the effect of the other. In addition, the activation of each pathway may be caused only by specific pairing; that is, pairing with positive timing activates the kinase-dependent P process, whereas pairing with negative timing activates the phosphatase-dependent D process. Such specificity may arise from the requirements for highly local and dynamic calcium signaling during STDP induction.

Dominance of potentiation in STDP integration

The amount of STDP that is induced by spike pairs depends on the spike timing interval[10,13]. This offered us an opportunity to investigate the role of induction strength in the integration of P and D using triplets with different spike timing intervals (**Fig. 4**). In this set of experiments, we selected spike timing of ±5 ms for the activation of strong P or D and ±15 ms for the activation of weak P or D. Of the four triplet paradigms, pre-post-pre {+15, –5} and {+5, –15} and post-pre-post {–5, +15} and {–15, +5}, three resulted in potentiation (**Fig. 4**). The potentiation induced by the post-pre-post triplet {–5, +15} indicated that weak P could overcome strong D when P was activated later (**Fig. 4c**,**e**). On the other hand, even when D was activated later, weak D could not negate strong P (**Fig. 4b**,**f**). These results indicate that P is dominant in the integration. It is also notable that triplet {+15, –5} did not produce pronounced depression but resulted in cancellation of potentiation and depression that was quantitatively similar to triplets {+10, –10} and {+5, –5} (see also **Fig. 6c**). Therefore, even in situations where P was not dominant, P and D did not linearly sum but resulted in cancellation.

Asymmetric integration with quadruplet stimuli

Because the pre-post-pre triplet involves two presynaptic spikes, short-term synaptic plasticity could in principle influence the outcome of STDP integration. At the culture stages used in these studies, however, most synapses in these hippocampal neurons showed moderate paired-pulse depression, and the paired-pulse ratio was uncorrelated with observed changes in synaptic strength (**Supplementary Fig. 2**). If the integration of P and D is assumed to be linear, paired-pulse depression should lead to more potentiation by pre-post-pre triplets than by post-pre-post triplets, the opposite of our experimental observation. Therefore, our results probably reflect nonlinearity in the interaction. To further evaluate this, we used quadruplet configurations that consist of two spike pairs (with spike timing of ±5 ms) separated by an interval T (defined as the time interval from the midpoint of the D-inducing spike pair to the midpoint of the P-inducing pair; T is positive when P follows D and negative when P precedes D; **Fig. 5**). Like the triplet configurations, quadruplet pre-post-post-pre induced little long-term synaptic change, whereas quadruplet post-pre-pre-post induced pronounced LTP (**Fig. 5**). Therefore, the integration of P and D in quadruplet paradigms follows the same rule as in triplets: P and D cancel when P is induced first, whereas P dominates when it is induced second.

Dependence of integration on initial synaptic strength

In our culture system, there is notable heterogeneity in the strength of synaptic connections. Previous studies in the same system have shown that the amount of spike-timing-dependent LTP, but not LTD, depends on the initial synaptic strength[13]. To evaluate how initial strength influences the outcome of STDP integration, we plotted the measured STDP ratio in individual triplet and quadruplet experiments against initial excitatory postsynaptic current (EPSC) size. A negative correlation between the STDP ratio and the initial EPSC amplitude was found in experiments using LTP-inducing triplet or quadruplet paradigms: considerably more potentiation was induced in initially weaker synapses (**Fig. 6a**). It is also notable that no correlation was found between STDP ratio and initial strength in experiments using paradigms that were ineffective at inducing LTP (**Fig. 6a**). Because LTP (but not LTD) that was induced by paired

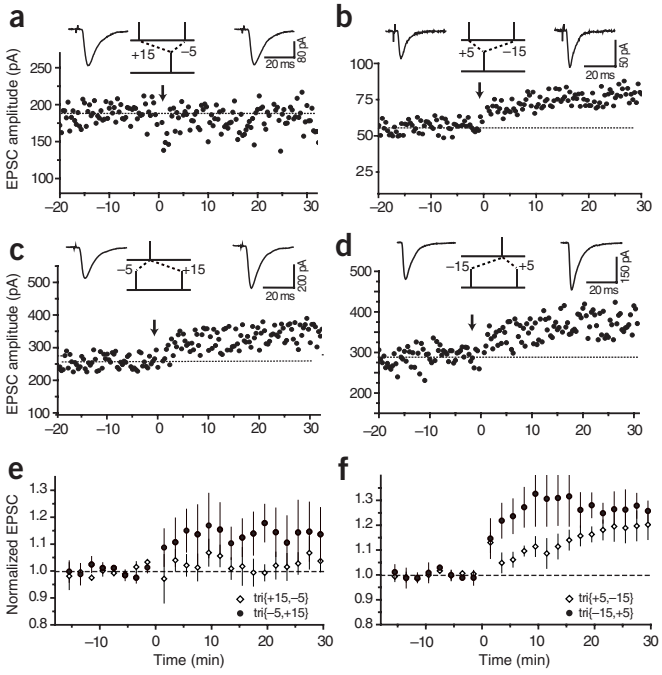

Figure 4 STDP integration after biased triplets with unequal positive and negative timings suggests dominant role of potentiation. (**a–d**) Results from typical experiments with (**a**) pre-post-pre triplet {+15, –5}, (**b**) pre-post-pre triplet {+5, –15}, (**c**) post-pre-post triplet {–5, +15} and (**d**) post-pre-post triplet {–15, +5}. (**e**) Summary of triplet experiments pre-post-pre {+15, –5) ($n = 7$) and post-pre-post {–5, +15} ($n = 6$). (**f**) Summary of triplet experiments pre-post-pre {+5, –15} ($n = 6$) and post-pre-post {–15, +5} ($n = 5$). Error bars, s.e.m.

spiking depended on initial synaptic strength, the cancellation of potentiation and depression that was independent of initial strength and that occurred during the ineffective triplet or quadruplet paradigms further indicates that the two processes do not integrate by linear summation.

Based on the dependence of potentiation on initial strength (**Fig. 6a**), we normalized the measured STDP ratio for experiments with potentiation-inducing paradigms (**Fig. 6b**,**c**). The normalized STDP ratio reduced the bias in the measurement that was due to the initial strength variability. Comparing the quantitative results from triplet and quadruplet experiments with opposite orders of effective P or D induction—triplet {+10, –10} versus triplet {–10, +10}, triplet {+5, –5} versus triplet {–5, +5} and quadruplet {$T = +25$} versus quadruplet {$T = –25$; **Fig. 6c**}—it is clear that temporal asymmetry is a general feature of STDP integration.

The L-type channel is needed for spike-timing-dependent LTD but not LTP[13]. Thus, we examined whether L-type channels are involved in the integration of P and D. In the presence of nimodipine, an L-type calcium channel antagonist, both the pre-post-pre triplet {+5, –5} and the post-pre-post triplet {–5, +5} resulted in similar amounts of LTP (**Fig. 6c**). The case of pre-post-pre triplet {+5, –5} is particularly telling, because specific blockade of calcium influx through L-type channels (thus less total calcium influx) resulted in potentiation, in contrast to the cancellation observed in the absence of drug. This suggests that specific calcium sources, and thus the spatial and temporal patterns of calcium transients at the synapse, are of critical importance in the induction and integration of STDP.

Dependence of integration on P and D activation timing

Comparing the amount of LTP induced by quadruplet post-pre-pre-post {+20} to that induced by the two post-pre-post triplets {–10, +10} and {–5, +5} (**Fig. 6b**,**c**), it is apparent that the quadruplet induced less LTP ($P = 0.016$, t-test). One possibility is that nonlinear integration of P and D depends on the time interval between P and D; the 25-ms interval (T) used in the quadruplet was longer than that in the triplet cases. To obtain a more complete picture of the timing dependence of this integration, we carried out more quadruplet experiments with spike timing of ±5 ms for the P- or D-inducing spike pairs and T varying from –105 to +105 ms. P and D canceled for all negative T values (pre-post-post-pre quadruplets) regardless of the interval (average synaptic change, 1.2 ± 1.8%; $n = 29$). This is similar to the triplet results (1.4 ± 1.8%; $n = 18$; **Fig. 7**). For positive T (post-pre-pre-post quadruplets), however, the integration depended on the time interval. When T was small, marked LTP (18.1 ± 2.7% for $T < 50$ ms; $n = 22$) resulted from a dominating P as in the triplet situations (27.4 ± 3.3%; $n = 14$). P and D seemed to cancel when T was longer, resulting in no change (3.6 ± 3.0% for $T > 70$ ms, $n = 6$).

The most notable feature in this summary (**Fig. 7**) is that P dominates the interaction when it follows D (hereafter referred to as D→P interaction) within a window of 70 ms. At a phenomenological level, this can be formulated as supralinear summation, with a 'history-dependent' term of extra potentiation that depends on the strength of P and D (denoted as P and D, respectively) and decays with increasing D→P interval T: $\delta(\text{D}\rightarrow\text{P}, T) = \alpha \times P \times D \times \exp(-T/\tau)$. Thus, the unitary change in synaptic weight (w) that is due to the integration is $\Delta w = D + P + \delta(\text{D}\rightarrow\text{P}, T)$. Here, exponential decay was chosen for simplicity, with the time

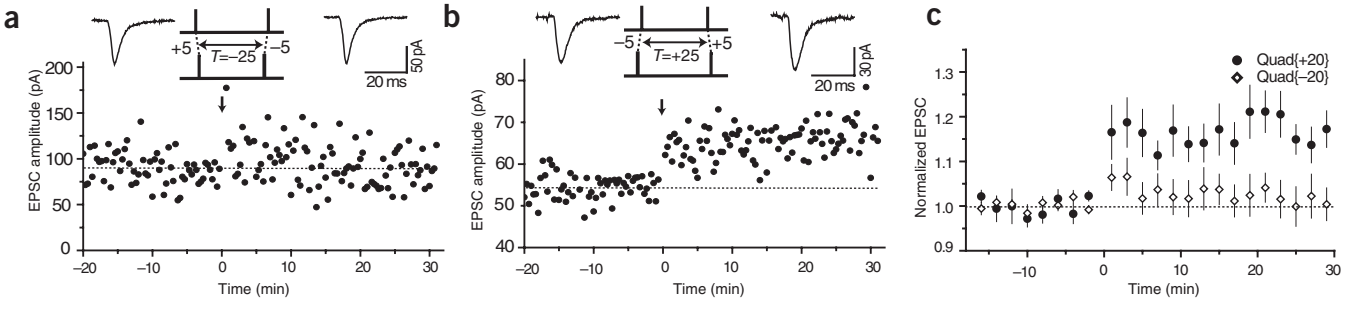

Figure 5 Asymmetric integration follows quadruplet stimuli. A quadruplet paradigm consisted of two spike pairs with ±5-ms spike timing that were separated by a longer interpair interval, T. (**a**) Result from a typical quadruplet experiment with $T = –25$ ms. (**b**) Result from a typical quadruplet experiment with $T = +25$ ms. (**c**) Summary of all quadruplet experiments with $T = +20$ to $+25$ ms (Quad{+20}; $n = 9$) and $T = –20$ to $–25$ms (Quad{–20}; $n = 10$). Error bars, s.e.m.

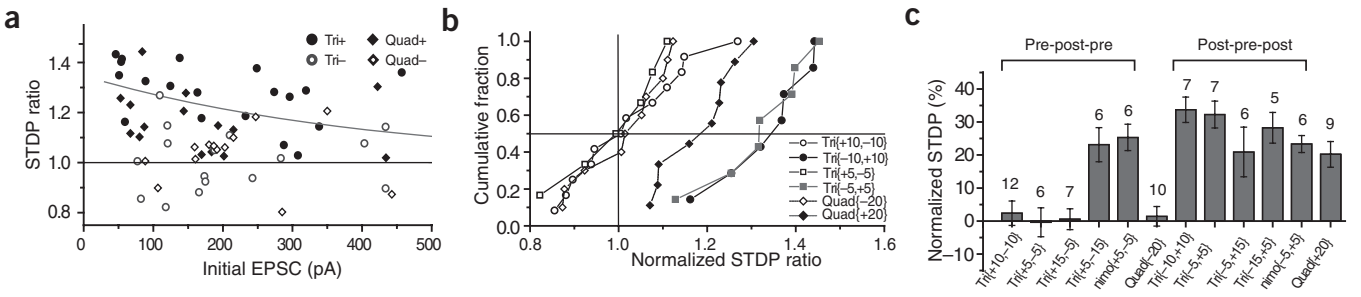

Figure 6 Normalization of STDP integration. (**a**) Dependence on initial strength in integration. Tri+ included data from experiments using post-pre-post triplets {–10, +10}, {–5, +5} and {–15, +5}. Tri– included data from experiments using pre-post-pre triplets {+10, –10}, {+5, –5} and {+15, –5}. Quad+ included quadruplet experiments with $0 < T < 25$ ms. Quad– included quadruplet experiments with $T < 0$. All Tri+ and Quad+ data were used to fit a single exponential curve $R = 1 + R1 \times e^{-A/A1}$ (R, STDP ratio; A, initial EPSC amplitude). Fitting result: $R1 = 0.33 \pm 0.05$; $A1 = 428 \pm 196$ pA (χ^2/degrees of freedom = 0.015; $R^2 = 0.14$). (**b**) Cumulative histogram of normalized STDP ratio for quadruplet and triplet experiments. Based on the actual initial EPSC amplitude (A) and the curve fit parameters ($R1 = 0.33$, $A1 = 428$), a correction value $\varepsilon = R1 \times (e^{-A/A1} - e^{-100/A1})$ was calculated as the predicted deviation of the STDP ratio from that for a fixed initial strength of 100 pA. Normalized STDP ratio was the measured STDP ratio after subtracting ε. Quad{+20} and Quad{–20} included the same dataset as in **Figure 5c**. (**c**) Summary of mean normalized STDP (in percent change) under different triplet and quadruplet conditions. Also included are results from experiments performed in the presence of nimodipine (nimo, 20 μM) using triplets {–5, +5} and {+5, –5}. Number of experiments in each data set is shown above each column. Error bars, s.e.m.

constant τ (~70 ms) derived from the right half of the timing window of the P and D interaction (**Fig. 7**). A scaling factor, α, can be chosen so that when P and D are both maximally activated, δ cancels D, resulting in $\Delta w = P$. For P→D integration, the left half of the timing window (**Fig. 7**) indicates that the two modules tend to cancel. In principle, this nonlinearity could be formulated as a set of nonlinear filters that allow previously activated P to influence subsequent D. Alternatively, the cancellation may reflect intrinsic instability of P and D modules (or subsequent signals), which can be implemented by additional terms that gate the effects of the modules.

DISCUSSION

Rules of STDP integration

Experimental studies of STDP have shown characteristic spike timing dependence that to a large extent is consistent across systems and preparations[10–19,35,36]. This property, in the form of various spike timing windows, can be regarded as a first-order rule because it describes the effects of simple paradigms in which only a single event of pre- and postsynaptic spike pairing could occur within the timescale of tens of milliseconds. To encompass more realistic activity patterns involving multiple pre- and postsynaptic spikes, most STDP models assume simple second-order rules for the integration of STDP, such as linear summation[22–26,37]. Our results, however, indicate that nonlinear second-order rules of STDP integration may occur, a consideration of which is likely to improve predictions of synaptic modifications that result from naturalistic spike trains. Nonetheless, these rules are likely to represent only part of the complexity of STDP integration. Other issues, for example, whether only near-neighbor spike interactions count, remain to be addressed[38]. Further, it is not clear whether more-complex spike patterns may engage additional (higher-order) rules. Ultimately, these issues will be resolved through better understanding of the underlying molecular signaling mechanisms.

The domination of P in D→P integration that we observed in hippocampal neurons is in opposition to the 'first-spike-dominating' rule—the spike that occurs first suppresses the efficacies of later spikes—that is found in layer 2/3 of the visual cortex[19]. One explanation is that layer 2/3 neurons may use additional mechanisms, such as strong short-term depression in both synaptic transmission and the back-propagation of action potentials, which in turn function as gates to limit downstream interaction between P and D from occurring in these synapses and to assure the priority of the earlier spike pairs. In other words, the first-spike-dominating rule may describe the interaction between adjacent spikes, whereas the timing-dependent integration of P and D reflects the properties of downstream signaling processes. Notably, in layer 5 of the visual cortex, STDP integration seems to follow an LTP-dominating rule[18]. Intuitively, our observations in cultured hippocampal neurons predict that with naturalistic spike train stimuli, LTP would also dominate when the spike rate is high. In the present study, however, the dominance of LTP is at least in part due to the detection of a specific temporal structure (such as D→P triplets and quadruplets) in the spike trains. Therefore, in contrast to the generality of the first-order rule of STDP that emphasizes causality detection as a fundamental neural function, multiple forms of the second-order rule may be 'tuned' to serve specific functions in different circuits.

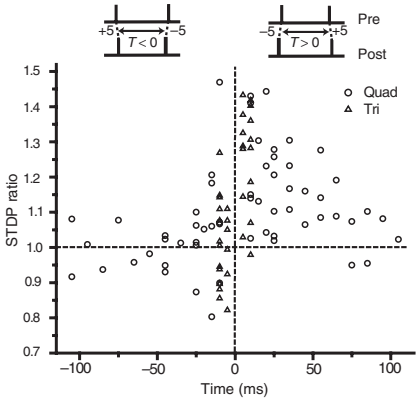

Figure 7 Asymmetric time window of STDP integration. Only quadruplet and triplet experiments with unbiased timing were included. STDP ratio and T were defined as in previous figures. Results from quadruplet experiments with smaller T were consistent with those from triplet experiments. For experiments with larger T, quadruplet results showed a 70-ms window within which potentiation dominates. Outside this window, potentiation and depression appeared to cancel each other.

Calcium signaling in STDP

At the cellular level, timing-dependent P and D integration underscores the dynamic nature of the intracellular signaling that underlies STDP. In accord with classical studies of LTP and LTD[5–7], our results indicate that

calcium and subsequent kinase and phosphatase pathways are crucial for STDP induction and integration. Several aspects of P and D integration that we observed, however, contradict the classical picture that the postsynaptic calcium increase dictates the outcome of synaptic potentiation or depression[28,31,39]. For example, whereas pre-post spike pairs induced LTP, most pre-post-pre triplets and pre-post-post-pre quadruplets that were tested did not result in substantial potentiation, as if the extra calcium influx that was triggered by the second presynaptic (and postsynaptic) stimulation had a negative impact. In addition, blocking L-type calcium channels allowed the pre-post-pre triplet to induce LTP, indicating a negative role for calcium influx from these channels. Therefore, in agreement with findings that classical LTP and LTD may depend on the duration of calcium elevation[40] and on the activation of specific receptor subunits[41], our results underscore the notion that when and where calcium influx occurs may be more critical than the amount of calcium increase for STDP. In other words, if postsynaptic calcium signals the induction of STDP, it must do so with its spatiotemporal dynamics at millisecond and submicron resolution. Such specificity may arise from the highly organized complexity of the postsynaptic density and nearby structures[42–44]. Ca^{2+} influxes from different channels seem to preferentially activate different kinase signaling pathways[45–47]. This could be due to the physical proximity of specific kinases to specific channels and/or distinct contributions of different channels to the temporal dynamics of intracellular Ca^{2+} transients. Indeed, with incorporation of multiple enzymatic pathways to detect the temporal profiles of calcium influx, a conductance-based biophysical model can reproduce the spike timing window and the asymmetric integration of STDP[48].

Modular activation and dynamic interaction of P and D

Our results demonstrate that, downstream of calcium, the CaMKII-dependent P signal and the calcineurin-dependent D signal were coactivated by multiple spike paradigms because pharmacological inhibition of either signal led to the expression of the other. Meanwhile, pairing paradigms with either positive or negative spike timing activated only the P signal or the D signal, respectively. Therefore, these early signaling processes can be regarded as relatively independent modules. Such modularity in plasticity signaling validates the basic assumption in mathematical models that the effect of complex spike trains can be decomposed into multiple pairing events[22–26]. During the induction of STDP, these modules may act as detectors of specific features in the spatiotemporal dynamics of calcium elevation resulting from pre- and postsynaptic spiking. The exact molecular mechanisms that underlie such detection remain to be identified. The 70-ms time window for P to override previously activated D does, however, indicate that the two modules are likely to reside in the same compartment where they interact nonlinearly over a timescale of tens of milliseconds.

Timing-dependent supralinear D→P integration may reflect the existence of cellular processes that allow D to sensitize subsequent P; this sensitization decays over time. Alternatively, it may also result from a slowly developing D that is interrupted by the activation of P. In either scenario, the dominating effect of P diminishes as the D→P interval increases. It should also be noted that during the induction period, the triplet or quadruplet paradigm was repeated at 1-s intervals for 1 min. Therefore with longer T, the D→P integration will be more or less equivalent to the P→D integration, in which P and D cancel. In other words, the result of cancellation at long intervals is consistent with the periodic stimulation paradigm. It is also notable that the cancellation in P→D integration is reminiscent of the depotentiation observed in various preparations[49], as well as the reversal of LTP and LTD under physiological conditions *in vivo*[50]. These phenomena at different timescales may reflect a certain intrinsic instability of the molecular signals that underlie the induction of LTP.

Implications for network function

How may the cellular properties of the interaction between P and D influence the computational functions of neuronal networks? In principle, the second-order rule could result in selective potentiation of synapses in response to stimuli with specific temporal structures. Even in the presence of noncorrelated background activity, however, the overall dominance of P in the P and D interaction could drive synapses to saturation. This undesirable consequence is likely to be prevented by the initial-strength dependence of potentiation (**Fig. 6a**). Because multiplicative potentiation but not depression decreases with increasing 'present' strength[13], weak synapses are more easily potentiated and strong synapses are more easily depressed. With such 'soft ceilings' for first-order STDP, noncorrelated background firing leads to a unimodal equilibrium distribution of synaptic weights[23,24,26]; the involvement of second-order interaction between P and D may shift the equilibrium to a higher mean value but is unlikely to cause saturation. Further, at low frequency, nonstructured spike patterns could rarely trigger supralinear D→P integration, because the D→P interval is likely to fall outside the 70-ms window. Meanwhile, frequent P and D cancellation may limit diffusion-like drift of synaptic weights that is caused by the random coincidence of pre- and postsynaptic firing, thereby improving the stability and reliability of the network.

METHODS

Cell culture. Low-density cultures of dissociated embryonic rat hippocampal neurons were prepared according to a previously described protocol with minor modifications[13], as approved by the University of Pittsburgh Institutional Animal Care and Use Committee. Hippocampi were removed from embryonic day (E) 17–18 rats and were treated with trypsin for 20 min at 37 °C, followed by washing and gentle trituration. The dissociated cells were plated on poly-L-lysine-coated glass coverslips in 35-mm Petri dishes with 30,000–60,000 cells per dish. The culture medium was Dulbecco's minimum essential medium (DMEM; BioWhittaker) supplemented with 10% heat-inactivated bovine calf serum (Hyclone), 10% Ham's F12 with glutamine (BioWhittaker), 50 U/ml penicillin-streptomycin (Sigma) and 1× B-27 (Invitrogen/Gibco). One-third of the culture medium was replaced with the same medium supplemented with 20 mM KCl 24 h after plating. Cytosine arabinoside (Sigma) was added to the culture dish (final concentration, 5 μM) around 7–10 days *in vitro* (DIV) to prevent overgrowth of glial cells. The optimal period for using these cultures is 8–15 DIV, during which glutamatergic connections of 50–500 pA are commonly found.

Electrophysiological recordings. Simultaneous whole-cell perforated-patch recordings were carried out with patch-clamp amplifiers (PC505A; Warner Instruments) at room temperature. The pipette solution contained the following: 136.5 mM K-gluconate, 17.5 mM KCl, 9 mM NaCl, 1 mM $MgCl_2$, 10 mM HEPES, 0.2 mM EGTA and 200 μg/ml amphotericin B (pH 7.3). The external bath solution was a HEPES-buffered saline (HBS): 150 mM NaCl, 3 mM KCl, 3 mM $CaCl_2$, 2 mM $MgCl_2$, 10 mM HEPES and 5 mM glucose (pH 7.3). Stock solutions of KN-62 (Calbiochem), CsA (Calbiochem) and nimodipine (Sigma/RBI) were first prepared in DMSO and then diluted (1:1,000) in HBS when being used. Throughout the recording, the culture was perfused with fresh bath solution at a constant rate of about 1 ml/min. Signals (filtered at 5 kHz) were acquired at a sampling rate of 10 kHz using a 16-bit digitizing board (E6035; National Instruments) interfaced with a custom program based on LabView (National Instruments), Igor Pro (WaveMetrics) or MatLab (MathWorks). Series resistances (10–30 MΩ) and input impedance (300–500 MΩ) were monitored by a test hyperpolarizing pulse (5 mV, 100 ms). Data were accepted for analysis only in the cases where series resistance and input impedance did not vary beyond 10% throughout the experiment. Trials showing significant run-up or run-down during the control period (>5% in 10 min) were also excluded from further analysis.

To minimize the complication of connectivity with other neurons that were not monitored by our recording, we examined only pairs of neurons that were found on isolated patches of glial cells. Neighboring neurons that may have been connected to the pair were removed with a suction pipette. Only monosynaptic connections between two glutamatergic neurons were included in the current

study. Polysynaptic connections were identified based on the latency of EPSC or inhibitory postsynaptic current onset (>5 ms) and were excluded from the study because their activation timing could not be precisely controlled. The STDP ratio was calculated from the averaged EPSC amplitude during two time periods: within 10 min before and between 15 and 30 min after the stimulation paradigm.

ACKNOWLEDGMENTS

We thank P. Lau for providing data for some STDP experiments; E. Aizenman, K. Kandler, P. Lau and J. Rubin for comments on the manuscript and members of the Bi lab for discussions. This work was supported by grants from Burroughs Wellcome Fund (Career Award in the Biomedical Sciences) and the National Institute of Mental Health (R01 MH066962) to G.Q.B.

Note: Supplementary information is available on the Nature Neuroscience website.

COMPETING INTERESTS STATEMENT

The authors declare that they have no competing financial interests.

Received 13 October; accepted 20 December 2004
Published online at http://www.nature.com/natureneuroscience/

1. Bliss, T.V. & Lømo, T. Long-lasting potentiation of synaptic transmission in the dentate area of the anaesthetized rabbit following stimulation of the perforant path. *J. Physiol. (Lond.)* **232**, 331–356 (1973).
2. Hebb, D.O. *The Organization of Behavior* (Wiley, New York, 1949).
3. Constantine-Paton, M., Cline, H.T. & Debski, E. Patterned activity, synaptic convergence, and the NMDA receptor in developing visual pathways. *Annu. Rev. Neurosci.* **13**, 129–154 (1990).
4. Bi, G.-Q. & Poo, M.-M. Synaptic modifications by correlated activity: Hebb's postulate revisited. *Annu. Rev. Neurosci.* **24**, 139–166 (2001).
5. Bliss, T.V. & Collingridge, G.L. A synaptic model of memory: long-term potentiation in the hippocampus. *Nature* **361**, 31–39 (1993).
6. Linden, D.J. & Connor, J.A. Long-term synaptic depression. *Annu. Rev. Neurosci.* **18**, 319–357 (1995).
7. Malenka, R.C. & Nicoll, R.A. Long-term potentiation—a decade of progress. *Science* **285**, 1870–1874 (1999).
8. Abbott, L.F. & Nelson, S.B. Synaptic plasticity: taming the beast. *Nat. Neurosci.* **3** (Suppl.), 1178–1183 (2000).
9. Sjostrom, P.J. & Nelson, S.B. Spike timing, calcium signals and synaptic plasticity. *Curr. Opin. Neurobiol.* **12**, 305–314 (2002).
10. Markram, H., Lubke, J., Frotscher, M. & Sakmann, B. Regulation of synaptic efficacy by coincidence of postsynaptic APs and EPSPs. *Science* **275**, 213–215 (1997).
11. Magee, J.C. & Johnston, D. A synaptically controlled, associative signal for Hebbian plasticity in hippocampal neurons. *Science* **275**, 209–213 (1997).
12. Mehta, M.R., Barnes, C.A. & McNaughton, B.L. Experience-dependent, asymmetric expansion of hippocampal place fields. *Proc. Natl. Acad. Sci. USA* **94**, 8918–8921 (1997).
13. Bi, G.-Q. & Poo, M.-M. Synaptic modifications in cultured hippocampal neurons: Dependence on spike timing, synaptic strength, and postsynaptic cell type. *J. Neurosci.* **18**, 10464–10472 (1998).
14. Debanne, D., Gahwiler, B.H. & Thompson, S.M. Long-term synaptic plasticity between pairs of individual CA3 pyramidal cells in rat hippocampal slice cultures. *J. Physiol. (Lond.)* **507**, 237–247 (1998).
15. Zhang, L.I., Tao, H.W., Holt, C.E., Harris, W.A. & Poo, M.-M. A critical window for cooperation and competition among developing retinotectal synapses. *Nature* **395**, 37–44 (1998).
16. Nishiyama, M., Hong, K., Mikoshiba, K., Poo, M.-M. & Kato, K. Calcium release from internal stores regulates polarity and input specificity of synaptic modification. *Nature* **408**, 584–588 (2000).
17. Feldman, D.E. Timing-based LTP and LTD at vertical inputs to layer II/III pyramidal cells in rat barrel cortex. *Neuron* **27**, 45–56 (2000).
18. Sjostrom, P.J., Turrigiano, G.G. & Nelson, S.B. Rate, timing, and cooperativity jointly determine cortical synaptic plasticity. *Neuron* **32**, 1149–1164 (2001).
19. Froemke, R.C. & Dan, Y. Spike-timing-dependent synaptic modification induced by natural spike trains. *Nature* **416**, 433–438 (2002).
20. Stevens, C.F. Strengths and weaknesses in memory. *Nature* **381**, 471–472 (1996).
21. Berninger, B. & Bi, G.-Q. Synaptic modification in neural circuits: A timely action. *Bioessays* **24**, 212–222 (2002).
22. Song, S., Miller, K.D. & Abbott, L.F. Competitive Hebbian learning through spike-timing-dependent synaptic plasticity. *Nat. Neurosci.* **3**, 919–926 (2000).
23. van Rossum, M.C., Bi, G.-Q. & Turrigiano, G.G. Stable hebbian learning from spike timing-dependent plasticity. *J. Neurosci.* **20**, 8812–8821 (2000).
24. Rubin, J., Lee, D.D. & Sompolinsky, H. Equilibrium properties of temporally asymmetric Hebbian plasticity. *Phys. Rev. Lett.* **86**, 364–367 (2001).
25. Senn, W. & Buchs, N.J. Spike-based synaptic plasticity and the emergence of direction selective simple cells: mathematical analysis. *J. Comput. Neurosci.* **14**, 119–138 (2003).
26. Gutig, R., Aharonov, R., Rotter, S. & Sompolinsky, H. Learning input correlations through nonlinear temporally asymmetric Hebbian plasticity. *J. Neurosci.* **23**, 3697–3714 (2003).
27. Hopfield, J.J. & Brody, C.D. Learning rules and network repair in spike-timing-based computation networks. *Proc. Natl. Acad. Sci. USA* **101**, 337–342 (2004).
28. Lisman, J. A mechanism for the Hebb and the anti-Hebb processes underlying learning and memory. *Proc. Natl. Acad. Sci. USA* **86**, 9574–9578 (1989).
29. Malenka, R.C. *et al.* An essential role for postsynaptic calmodulin and protein kinase activity in long-term potentiation. *Nature* **340**, 554–557 (1989).
30. Malinow, R., Schulman, H. & Tsien, R.W. Inhibition of postsynaptic PKC or CaMKII blocks induction but not expression of LTP. *Science* **245**, 862–866 (1989).
31. Artola, A. & Singer, W. Long-term depression of excitatory synaptic transmission and its relationship to long-term potentiation. *Trends Neurosci.* **16**, 480–487 (1993).
32. Mulkey, R.M., Endo, S., Shenolikar, S. & Malenka, R.C. Involvement of a calcineurin/inhibitor-1 phosphatase cascade in hippocampal long-term depression. *Nature* **369**, 486–488 (1994).
33. Lisman, J., Schulman, H. & Cline, H. The molecular basis of CaMKII function in synaptic and behavioural memory. *Nat. Rev. Neurosci.* **3**, 175–190 (2002).
34. Ito, I., Hidaka, H. & Sugiyama, H. Effects of KN-62, a specific inhibitor of calcium/calmodulin-dependent protein kinase II, on long-term potentiation in the rat hippocampus. *Neurosci. Lett.* **121**, 119–121 (1991).
35. Yao, H. & Dan, Y. Stimulus timing-dependent plasticity in cortical processing of orientation. *Neuron* **32**, 315–323 (2001).
36. Schuett, S., Bonhoeffer, T. & Hubener, M. Pairing-induced changes of orientation maps in cat visual cortex. *Neuron* **32**, 325–337 (2001).
37. Izhikevich, E.M. & Desai, N.S. Relating STDP to BCM. *Neural Comput.* **15**, 1511–1523 (2003).
38. Bi, G.Q. Spatiotemporal specificity of synaptic plasticity: cellular rules and mechanisms. *Biol. Cybern.* **87**, 319–332 (2002).
39. Shouval, H.Z., Bear, M.F. & Cooper, L.N. A unified model of NMDA receptor-dependent bidirectional synaptic plasticity. *Proc. Natl. Acad. Sci. USA* **99**, 10831–10836 (2002).
40. Yang, S.N., Tang, Y.G. & Zucker, R.S. Selective induction of LTP and LTD by postsynaptic $[Ca^{2+}]_i$ elevation. *J. Neurophysiol.* **81**, 781–787 (1999).
41. Liu, L. *et al.* Role of NMDA receptor subtypes in governing the direction of hippocampal synaptic plasticity. *Science* **304**, 1021–1024 (2004).
42. Scannevin, R.H. & Huganir, R.L. Postsynaptic organization and regulation of excitatory synapses. *Nat. Rev. Neurosci.* **1**, 133–141 (2000).
43. Sheng, M. & Sala, C. PDZ domains and the organization of supramolecular complexes. *Annu. Rev. Neurosci.* **24**, 1–29 (2001).
44. Petersen, J.D. *et al.* Distribution of postsynaptic density (PSD)-95 and Ca^{2+}/calmodulin-dependent protein kinase II at the PSD. *J. Neurosci.* **23**, 11270–11278 (2003).
45. Graef, I.A. *et al.* L-type calcium channels and GSK-3 regulate the activity of NF-ATc4 in hippocampal neurons. *Nature* **401**, 703–708 (1999).
46. Dolmetsch, R.E., Pajvani, U., Fife, K., Spotts, J.M. & Greenberg, M.E. Signaling to the nucleus by an L-type calcium channel-calmodulin complex through the MAP kinase pathway. *Science* **294**, 333–339 (2001).
47. West, A.E. *et al.* Calcium regulation of neuronal gene expression. *Proc. Natl. Acad. Sci. USA* **98**, 11024–11031 (2001).
48. Rubin, J.E., Gerkin, R.C., Bi, G.-Q. & Chow, C.C. Calcium time course as a signal for spike-timing dependent plasticity. *J. Neurophysiol.* (in the press).
49. Zhou, Q. & Poo, M.M. Reversal and consolidation of activity-induced synaptic modifications. *Trends Neurosci.* **27**, 378–383 (2004).
50. Zhou, Q., Tao, H.W. & Poo, M.M. Reversal and stabilization of synaptic modifications in a developing visual system. *Science* **300**, 1953–1957 (2003).